



HAL
open science

Rogue waves in shallow water in the presence of a vertically sheared current

Christhian Kharif, Malek Abid, Julien Touboul

► **To cite this version:**

Christhian Kharif, Malek Abid, Julien Touboul. Rogue waves in shallow water in the presence of a vertically sheared current. *Journal of Ocean Engineering and Marine Energy*, 2017, 10.1007/s40722-017-0085-7 . hal-01579991

HAL Id: hal-01579991

<https://hal.science/hal-01579991>

Submitted on 19 Feb 2023

HAL is a multi-disciplinary open access archive for the deposit and dissemination of scientific research documents, whether they are published or not. The documents may come from teaching and research institutions in France or abroad, or from public or private research centers.

L'archive ouverte pluridisciplinaire **HAL**, est destinée au dépôt et à la diffusion de documents scientifiques de niveau recherche, publiés ou non, émanant des établissements d'enseignement et de recherche français ou étrangers, des laboratoires publics ou privés.

1 **Rogue waves in shallow water in the presence of a**
2 **vertically sheared current**

3 **Christian Kharif · Malek Abid · Julien**
4 **Touboul**

5
6 Received: date / Accepted: date

7 **Abstract** Two-dimensional rogue wave occurrence in shallow water on a vertically
8 sheared current of constant vorticity is considered. Using Euler equations and Rie-
9 mann invariants in the shallow water approximation, hyperbolic equations for the
10 surface elevation and the horizontal velocity are derived and closed-form nonlin-
11 ear evolution equation for the surface elevation is obtained. Following Whitham
12 (1974), a dispersive term is added to this equation using the fully linear disper-
13 sion relation. With this new single first-order partial differential equation, vorticity
14 effects on rogue wave properties are studied numerically. Besides, the Boundary
15 Integral Element Method (BIEM) and the KdV equation both with vorticity are
16 used for this numerical investigation, too. It is shown that results from the gen-
17 eralised Whitham equation agree quite well with those from BIEM whereas those
18 from the KdV model are quite different. The numerical simulations carried out
19 with the generalised Whitham equation and BIEM show that the presence of an
20 underlying vertically sheared current modifies rogue wave properties significantly.
21 For negative vorticity the amplification factor and duration of extreme wave events
22 are increased whereas it is the opposite for positive vorticity. Furthermore, the wave
23 amplification is larger when the current is opposing.

C. Kharif
Aix Marseille Université, CNRS, Centrale Marseille, IRPHE UMR 7342, F-13384, Marseille,
France
E-mail: kharif@irphe.univ-mrs.fr

M. Abid
Aix Marseille Université, CNRS, Centrale Marseille, IRPHE UMR 7342, F-13384, Marseille,
France

J. Touboul
Université de Toulon, Aix Marseille Université, CNRS, IRD, Mediterranean Institute of
Oceanography (MIO), La Garde, France
Aix Marseille Université, Université de Toulon, CNRS, IRD, Mediterranean Institute of
Oceanography (MIO), Marseille, France

1 Introduction

Generally, in coastal and ocean waters, current velocity profiles are established by bottom friction and wind stress at the sea surface, and consequently are vertically varying. Ebb and flood currents due to the tide may have an important effect on water wave properties. In any region where the wind blows, the generated current affects the behavior of the waves. The present work focuses on the nonlinear evolution of two-dimensional gravity waves propagating in shallow water on a shear current which varies linearly with depth. We assume that the directional spread of the wave field is sufficiently narrow to consider unidirectional propagation of the waves.

There are a number of physical mechanisms that focus the wave energy into a small area and produce the occurrence of extreme waves called freak or rogue waves. These events may be due to refraction (presence of variable currents or bottom topography), dispersion (frequency modulation), wave instability (the modulational instability), soliton interactions, crossing seas, etc. For more details on these different mechanisms see the reviews on freak waves by Kharif and Pelinovsky (2003), Dysthe et al (2008), Kharif et al (2009) and Onorato et al (2013). Few studies have been devoted to the occurrence of extreme wave events in shallow water. Among the authors who have investigated rogue wave properties in shallow water, one can cite Pelinovsky et al (2000) , Kharif et al (2000), Peterson et al (2003), Soomere and Engelbrecht (2005), Talipova et al (2008) and Chambarel et al (2010). Pelinovsky and Sergeeva (2006) and Toffoli et al (2006) investigated the statistical properties of rogue waves in shallow water.

To the best of our knowledge, there is no paper on the effect of a vertically sheared current on rogue wave properties apart from that of Touboul and Kharif (2016) in deep water. We propose to extend this work to the case of shallow water.

Within the framework of the shallow water wave theory Whitham (1974) proposed a generalised equation governing the evolution of fully nonlinear waves satisfying the full linear dispersion. The Whitham equation may be derived from the previous generalised Whitham equation assuming that the waves are weakly nonlinear. The Whitham equation and the KdV equation which have the same nonlinear term differ from each other by the dispersive term. Very recently, Hur & Johnson (2015) have considered a modified Whitham equation taking account of constant vorticity. Very recently, Kharif and Abid (2017) have proposed a new model derived from the Euler equations for water waves propagating on a vertically sheared current of constant vorticity in shallow water. The heuristic introduction of dispersion allows the study of strongly nonlinear two-dimensional long gravity waves in the presence of vorticity. Consequently, this new equation extends to waves propagating in the presence of vorticity the generalised Whitham equation.

Two different approaches are used to investigate rogue waves propagating in shallow water on a shear current of constant vorticity: the generalised Whitham equation with vorticity and the Boundary Integral Element Method (BIEM) which allows the study of fully nonlinear dispersive water waves on arbitrary depth in the presence of vorticity (see Touboul and Kharif (2016)). Besides, a numerical investigation is carried out by using the KdV equation with constant vorticity whose derivation can be found in the papers by Freeman and Johnson (1970) and Choi (2003). Note that the latter equation can be derived from the generalised

71 Whitham equation with vorticity assuming that the waves are weakly nonlinear
72 and weakly dispersive.

73 **2 Two mathematical formulations**

74 2.1 The generalised Whitham equation with vorticity

75 We consider two-dimensional gravity water waves propagating at the free surface
76 of a vertically sheared current of uniform intensity Ω which is the opposite of the
77 vorticity. The wave train moves along the x – axis and the z – axis is oriented
78 upward opposite to the gravity. The origin $z = 0$ is the undisturbed free surface
79 and $z = -h$ is the rigid horizontal bottom.

80 The continuity equation is

$$u_x + w_z = 0 \quad (1)$$

81 where u and w are the longitudinal and vertical components of the *wave induced*
82 *velocity*, respectively. The underlying current is $U = U_0 + \Omega z$ where U_0 is the
83 constant surface velocity.

84 Integrating equation (1) from the bottom to free surface gives

$$w(z = \eta) - w(z = -h) = u(z = \eta)\eta_x - \frac{\partial}{\partial x} \int_{-h}^{\eta(x,t)} u dz \quad (2)$$

85 The vertical component of the velocity at the free surface, $w(z = \eta)$, and at the
86 bottom, $w(z = -h)$, are obtained from the kinematic boundary condition and
87 bottom condition

$$w(z = \eta) = \eta_t + [u(z = \eta) + U_0 + \Omega\eta]\eta_x$$

88

$$w(z = -h) = 0$$

89 Consequently equation (2) becomes

$$\frac{\partial}{\partial x} \int_{-h}^{\eta(x,t)} u dz + (U_0 + \Omega\eta)\eta_x = 0$$

90 Assuming u to be independent of z , we obtain the following equation

$$\eta_t + \frac{\partial}{\partial x} [u(\eta + h) + \frac{\Omega}{2}\eta^2 + U_0\eta] = 0 \quad (3)$$

91

92 Equation (3) corresponds to mass conservation in shallow water in the presence of
93 constant vorticity.

94 The Euler equation in the x -direction is

$$u_t + (u + U_0 + \Omega z)u_x + \Omega w = -\frac{1}{\rho}P_x$$

95 with u independent of z and ρ the water density.

96 Using the hydrostatic assumption for the pressure

$$P = \rho g(\eta - z)$$

97 where g is the gravity.

98 The Euler equation in the x -direction is rewritten as follows

$$u_t + (u + U_0 + \Omega z)u_x + \Omega w + g\eta_x = 0 \quad (4)$$

99

100 Using the continuity equation and boundary conditions that w satisfies on the
101 bottom and at the free surface, we obtain

$$w = -(z + h)u_x \quad (5)$$

102 Finally, the Euler equation becomes

$$u_t + (u + U_0 - \Omega h)u_x + g\eta_x = 0 \quad (6)$$

103 The dynamics of non dispersive shallow water waves on a vertically sheared cur-
104 rent of constant vorticity is governed by equations (3) and (6) that admit a pair of
105 Riemann invariants. These Riemann invariants which are derived analytically al-
106 lows us to express the longitudinal component of the wave induced velocity $u(x, t)$
107 as a function of the elevation η . Finally, equations (3) and (6) can be reduced to
108 the following single nonlinear partial differential equation for η

$$\eta_t + \left\{ U_0 - \frac{\Omega h}{2} + 2\sqrt{g(\eta + h) + \Omega^2(\eta + h)^2/4} - \sqrt{gh + \Omega^2 h^2/4} \quad + \right. \\ \left. \frac{g}{\Omega} \ln \left[1 + \frac{\Omega}{2g} \frac{\Omega\eta + 2(\sqrt{g(\eta + h) + \Omega^2(\eta + h)^2/4} - \sqrt{gh + \Omega^2 h^2/4})}{1 + \frac{\Omega}{g}(\frac{\Omega h}{2} + \sqrt{gh + \Omega^2 h^2/4})} \right] \right\} \eta_x = 0 \quad (7)$$

109 More details on the derivation of this equation is given in the appendix. Equation
110 (7) is fully nonlinear and describes the spatio-temporal evolution of hyperbolic
111 water waves propagating rightwards in shallow water in the presence of constant
112 vorticity.

113 Following Whitham (1974), full linear dispersion is introduced heuristically

$$\eta_t + \left\{ U_0 - \frac{\Omega h}{2} + 2\sqrt{g(\eta + h) + \Omega^2(\eta + h)^2/4} - \sqrt{gh + \Omega^2 h^2/4} \quad + \right. \\ \left. \frac{g}{\Omega} \ln \left[1 + \frac{\Omega}{2g} \frac{\Omega\eta + 2(\sqrt{g(\eta + h) + \Omega^2(\eta + h)^2/4} - \sqrt{gh + \Omega^2 h^2/4})}{1 + \frac{\Omega}{g}(\frac{\Omega h}{2} + \sqrt{gh + \Omega^2 h^2/4})} \right] \right\} \eta_x + K * \eta_x = 0 \quad (8)$$

114 where $K * \eta_x$ is a convolution product. The kernel K is given as the inverse Fourier
115 transform of the fully linear dispersion relation of gravity waves in finite depth in
116 the presence of constant vorticity Ω : $K = F^{-1}(c)$ with

$$c = U_0 + \sqrt{gh} \left(\sqrt{\frac{\tanh(kh)}{kh} \left(\frac{\Omega^2 \tanh(kh)}{4gk} + 1 \right)} - \frac{\Omega \tanh(kh)}{2k\sqrt{gh}} \right) \quad (9)$$

117 The expression of the phase velocity given by equation (9) can be found in the
118 paper by Choi (2003).

Equation (8) governs the propagation of nonlinear long gravity waves in a fully linear dispersive medium. For $\Omega = 0$ and $U_0 = 0$, (7) reduces to generalised equation (13.97) of Whitham (1974).

For weakly nonlinear ($\eta/h \ll 1$) and weakly dispersive ($kh \ll 1$) waves, equation (8) reduces to the KdV equation with vorticity derived by Freeman and Johnson (1970) and Choi (2003) who used multiple scale methods, different to the approach used herein. To set the KdV equation in dimensionless form, h and $\sqrt{h/g}$ are chosen as reference length and reference time which corresponds to $h = 1$ and $g = 1$. The equation reads

$$\eta_t + c_0(\Omega)\eta_x + c_1(\Omega)\eta\eta_x + c_2(\Omega)\eta_{xxx} = 0 \quad (10)$$

with

$$c_0 = U_0 - \frac{\Omega}{2} + \sqrt{1 + \Omega^2/4} \quad , \quad c_1 = \frac{3 + \Omega^2}{\sqrt{4 + \Omega^2}} \quad , \quad c_2 = \frac{2 + \Omega^2 - \Omega\sqrt{4 + \Omega^2}}{6\sqrt{4 + \Omega^2}}$$

The equations (7), (8) and (10) are solved numerically in a periodic domain of length $2L$. The length L is chosen $O(400\delta)$ where δ is a characteristic length scale of the initial condition. The number of grid points is $N_x = 2^{12}$. Spatial derivatives are computed in the Fourier space and nonlinear terms in the physical space. The link between the two spaces is made by the Fast Fourier Transform. For the time integration, a splitting technique is used. The equations (7), (8) and (10) could be written as

$$\eta_t + L + N = 0, \quad (11)$$

where L and N are linear and nonlinear differential operators in η , respectively. Note that in general the operators L and N do not commute. If the initial condition is η_0 , the exact solution of the previous equation is

$$\eta(t) = e^{-(L+N)t}\eta_0. \quad (12)$$

This equation is discretized as follows. Let $t_n = n\Delta t$. We have

$$\eta(t_n) = e^{-(L+N)n\Delta t}\eta_0 = (e^{-L\Delta t/2}e^{-N\Delta t}e^{-L\Delta t/2})^n\eta_0 + O(\Delta t^2), \quad (13)$$

and the scheme is globally second order in time. The operator $e^{-L\Delta t/2}$ is computed exactly in the Fourier space. However, the operator $e^{-N\Delta t}$ is approximated using a Runge-Kutta scheme of order 4. The time step is chosen as $\Delta t = 0.005$. Furthermore, the efficiency and accuracy of the numerical method has been checked against the nonlinear analytical solution of the St-Venant equations for the dam-break problem in the absence of current and vorticity ($\Omega = 0$ and $U_0 = 0$). For $U_0 = 0$ and $\Omega = 0$ equation (7) reduces to

$$H_t + (3\sqrt{gH} - 2\sqrt{gh})H_x = 0, \quad \text{with } H = \eta + h. \quad (14)$$

For $t > 0$, the nonlinear analytical solution of equation (14) is

$$\begin{aligned} H(x, t) &= h, & u(x, t) &= 0; & \frac{x}{t} &\geq \sqrt{gh} \\ H(x, t) &= \frac{h}{9} \left(2 + \frac{x}{\sqrt{gh}t} \right)^2, & u(x, t) &= -\frac{2}{3} (\sqrt{gh} - \frac{x}{t}); & -2\sqrt{gh} &\leq \frac{x}{t} \leq \sqrt{gh} \\ H(x, t) &= 0, & u(x, t) &= 0; & \frac{x}{t} &\leq -2\sqrt{gh} \end{aligned} \quad (15)$$

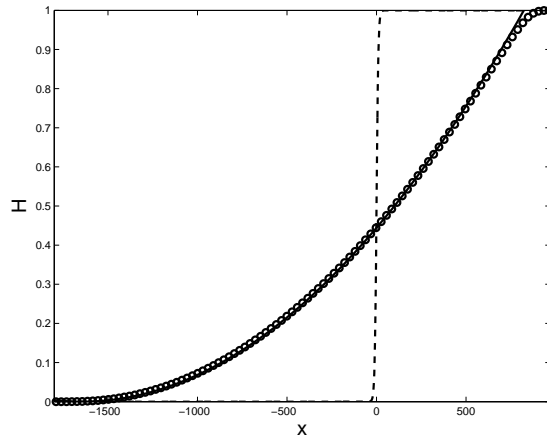


Fig. 1 Dam-break: comparison between analytical (solid line) and numerical solutions (\circ) after the dam has broken. The dashed line represents the initial condition at $t = 0$

149 At time $t = 0$ the initial condition is $H(x, 0) = h(1 + \tanh(2x))/2$ and $u(x, 0) = 0$
 150 everywhere. A numerical simulation of equation (14) has been carried out with
 151 $g = 1$ and $h = 1$. The numerical and analytical surface profiles at $t = 0$ and after
 152 the dam has broken are plotted in figure 1.

153 Within the framework of the KdV equation in the presence of vorticity, we have
 154 also checked that solitary waves are propagated with the right velocity that de-
 155 pends on Ω .

156 2.2 The boundary Integral Element Method

157 The problem considered here is identical to the one described in the previous sec-
 158 tion. It is two dimensional, and the current field is assumed to be steady, constant
 159 in the horizontal direction, and to vary linearly with depth,

$$U(z) = U_0 + \Omega z. \quad (16)$$

160 The three dimensional interaction of water waves propagating obliquely in the
 161 assumed current are not considered here. The vorticity within the flow is thus
 162 constant, as previously mentioned. It is straightforward that such current, associ-
 163 ated with hydrostatic pressure $P(z) = p_0 - gz$ is solution of the Euler equations
 164 when considering a problem of constant depth. This will allow to seek for wavy
 165 perturbations $(u(x, z, t), v(x, z, t))$ associated with the pressure field $p(x, z, t)$. The
 166 total flow fields are then given by

$$\begin{aligned} \tilde{u}(x, z, t) &= u(x, z, t) + U(z), \\ \tilde{v}(x, z, t) &= v(x, z, t) \quad \text{and} \\ \tilde{p}(x, z, t) &= p(x, z, t) + P(z). \end{aligned} \quad (17)$$

167 Using this decomposition, the Euler equations might reduce to

$$u_t + (U + u)u_x + vU_z + vu_z = -\frac{p_x}{\rho} \quad \text{and} \quad (18)$$

$$v_t + (U + u)v_x + vv_z + g = -\frac{p_z}{\rho}, \quad (19)$$

168 which has to be fulfilled together with the continuity equation

$$u_x + v_z = 0. \quad (20)$$

169 As it is demonstrated in Simmen (1984), and more recently in Nwogu (2009),
 170 the wavy perturbations propagating in such current conditions are irrotational.
 171 Indeed, since the second derivative of the background current U_{zz} is nil, the vor-
 172 ticity conservation equation involves no source term, and the vorticity field does
 173 not exchange any vorticity with the wavy perturbations. Thus, we might introduce
 174 a velocity potential $\phi(x, z, t)$ from which derive the perturbation induced veloci-
 175 ties ($\nabla\phi = (u, v)$). It has to be emphasized that the continuity equation (20) is
 176 automatically satisfied if the velocity potential is solution of Laplace's equation

$$\Delta\phi = 0. \quad (21)$$

177 The kinematic free surface condition might also be expressed, and if (X, Z) denotes
 178 the location of a particle at the free surface, this condition might be expressed

$$\frac{dX}{dt} = u \quad \text{and} \quad \frac{dZ}{dt} = v - U(\eta)\frac{\partial\eta}{\partial x}, \quad (22)$$

179 where d/dt refers to the material derivative $d/dt = \partial/\partial t + u\partial/\partial x + v\partial/\partial z$, and
 180 $Z = \eta(x, t)$.

181 Now, a stream function ψ can also be introduced, so that $(\partial\psi/\partial z, -\partial\psi/\partial x) =$
 182 (u, v) . The Euler equations (18) and (19) can now be integrated in space, and it
 183 comes

$$\frac{\partial\phi}{\partial t} + U(z)\frac{\partial\phi}{\partial x} + \frac{\nabla\phi^2}{2} - \Omega\psi + gz = -\frac{p}{\rho} \quad (23)$$

184 When applied to the free surface, where the pressure is constant, this equation pro-
 185 vides the classical dynamic boundary condition. Introducing the material deriva-
 186 tive used in the kinematic condition, this condition reduces to

$$\frac{d\phi}{dt} + U(\eta)\frac{\partial\phi}{\partial x} - \frac{\nabla\phi^2}{2} - \Omega\psi + g\eta = 0, \quad (24)$$

187 At this point, the knowledge of the stream function ψ at the free surface is still
 188 needed. Hopefully, one can notice the relationship

$$\frac{\partial\psi}{\partial\tau} = -\frac{\partial\phi}{\partial n}, \quad (25)$$

189 where $(\boldsymbol{\tau}, \mathbf{n})$ refer respectively to the tangential and normal vectors at the free
 190 surface. Thus, the stream function ψ can be evaluated at the free surface as soon
 191 as the normal derivative of the velocity potential is known.

192 Furthermore, if equations (22), (24) and (25) refer to the boundary condition at
 193 the free surface, the fluid domain still has to be closed. This is done by using
 194 impermeability conditions on the bottom boundary condition, located at $z = -h$,

195 h being used as the reference length (i.e. $h = 1$) and on the vertical boundary
 196 conditions, located respectively at $x = 0$ and $x = 200$.

197 The numerical approach used here has already been implemented and used
 198 successfully in the framework of focusing wave groups in the presence of uniform
 199 current (Touboul et al (2007); Merkoune et al (2013)). The extension allowing to
 200 take constant vorticity into account was presented in Touboul and Kharif (2016)
 201 together with a validation of the approach. It is based on a Boundary Integral
 202 Element Method (BIEM) coupled with a Mixed Euler Lagrange (MEL) procedure.
 203 At each time step, the Green's second identity is discretized to solve numerically
 204 the Laplace equation (21). Thus, the potential and its normal derivative are known
 205 numerically, and the stream function ψ can be deduced by integration of equation
 206 (25) along the free surface. This numerical integration is performed in the up-wave
 207 direction, starting from the down-wave end of the basin, and using zero as initial
 208 value. Then, the time stepping is performed by numerical integration of equations
 209 (22) and (24) using a fourth order Runge & Kutta scheme. Full details of the
 210 implementation can be found in Touboul and Kharif (2010). In every simulations,
 211 the total number of points considered at the free surface was $N_{fs} = 1000$, while
 212 the total number of points used on the solid boundaries was $N_{bo} = 600$. The time
 213 step used for the simulations was $dt = 0.01$.

214 2.3 Initial condition

215 Both numerical approaches described in previous subsections were initialised with
 216 the same initial condition. Following the approach described in Kharif et al (2000);
 217 Pelinovsky et al (2000), the initial condition is obtained numerically. A Gaussian
 218 initial wave, with no initial velocity, is allowed to collapse under gravity. This
 219 simulation is run in the absence of current and vorticity, using the BIEM. Two
 220 radiated wave trains, propagating in opposite directions, are generated. The wave
 221 group propagating in the $(-x)$ direction is isolated, and space-time coordinates
 222 are reverted. This allows the generation of a focusing wave group in shallow water
 223 conditions. For the numerical simulations considered here, the initial gaussian ele-
 224 vation has a maximum amplitude $a = h/2$ where h still being the reference length,
 225 and a width $\sigma = h/2\sqrt{2}$.

226 The wave train considered is used as initial condition for both numerical ap-
 227 proaches. The surface elevation of this focusing wave group is used as initial
 228 condition for the generalised-Whitham equation with vorticity, and for the KdV
 229 equation with vorticity as well. Both elevations and velocity potential are required
 230 to initialise the BIEM.

231 The dimensionless value of the maximum surface elevation of the wave group ob-
 232 tained, $\eta_{\max}(t = 0)$, is 0.0715. The dynamics of this wave packet is illustrated in
 233 figure 2, in the framework of BIEM simulations. The initial wave packet is propa-
 234 gated, and the effects of both nonlinearity and dispersion lead to the formation of
 235 a high wave. Figure 2 shows surface profiles of the wave group during the focusing
 236 and defocusing stages at several times. The rogue wave occurs at $t/T = 75$.

237 We have chosen an initial condition provided by the BIEM because the generalised
 238 Whitham and KdV equations cannot supply the velocity profile beneath the wave.
 239 The consequence to have imposed the same initial condition for the three different

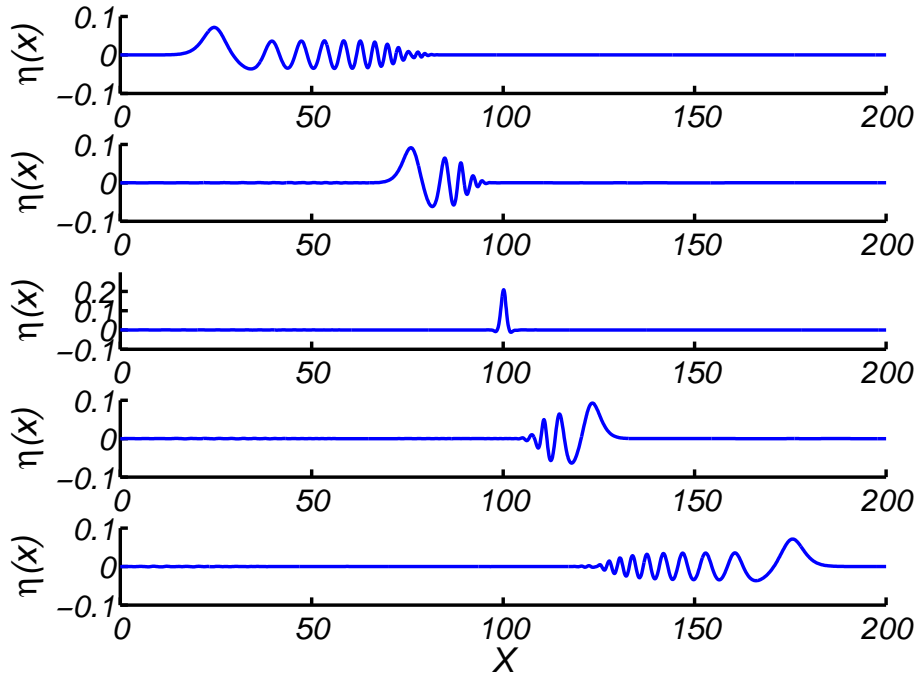


Fig. 2 Surface elevation of the focusing and defocusing wave group evolving. From top to bottom: ($t/T = 0$), ($t/T = 50$), ($t/T = 75$), ($t/T = 100$) and ($t/T = 150$).

240 models is that this initial condition is not optimal for the KdV and generalised
 241 Whitham equations.

242 3 Results and discussion

243 As KdV equation (10) and equations derived in subsection 2.2, equation (8) is set
 244 in dimensionless form by taking h and $\sqrt{h/g}$ as unit of length and time, respec-
 245 tively. In other words, we have imposed $h = 1$ and $g = 1$. The surface current, U_0 ,
 246 is ignored to only focus on vorticity effect. Consequently the underlying is $U = \Omega z$.
 247 Among the rogue wave properties, a particular attention is paid to the amplifica-
 248 tion factor of the maximum surface elevation, defined as $\eta_{\max}(t)/\eta_{\max}(t = 0)$. The
 249 time evolution of this amplification factor is plotted in figures 3-7 for several values
 250 of the shear Ω . One can see that the evolutions computed with the generalised
 251 Whitham equation and BIEM are similar even though the amplification is overes-
 252 timated with the generalised Whitham equation with vorticity. The amplification
 253 factor at the focusing time t_f plotted in figure 8 increases as the shear Ω increases.
 254 One can observe that the difference between the two curves decreases as the shear
 255 Ω increases. In other words, the agreement is better for positive values of the
 256 shear Ω (negative vorticity) than for negative values of Ω (positive vorticity). Like
 257 Grimshaw and Liu (2017) who considered a similar problem, we found that the
 258 wave growth is larger when the current is opposing. The KdV equation exhibits

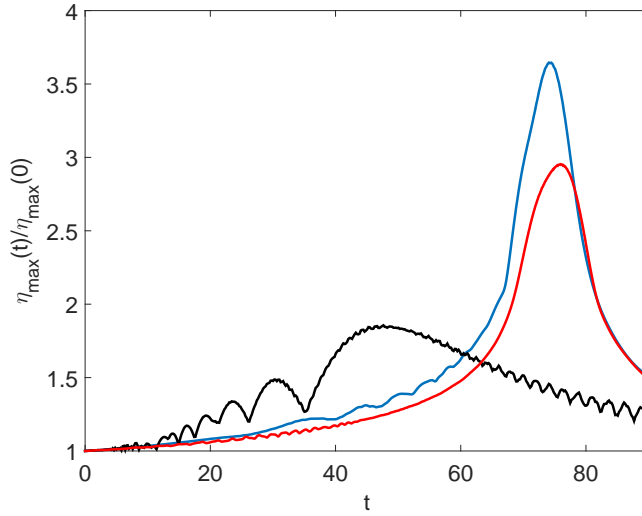


Fig. 3 (color online) Time evolution of the amplification factor without vorticity effect ($\Omega = 0$). Generalised Whitham equation (blue solid line), BIEM (red solid line) and KdV equation (black solid line)

259 the same tendency that is an increase of the maximum of amplification with Ω .
 260 The focusing time t_f obtained with both models are very close. On the opposite,
 261 the KdV equation underestimates the maximum value of the amplification factor
 262 and the focusing time t_f as well. In figures 6 and 7, the BIEM shows for negative
 263 values of the shear Ω first a reduction of the maximum surface elevation and then
 264 an amplification. This attenuation of the maximum of the surface elevation does
 265 not occur for the generalised Whitham and KdV equations. We define as extreme
 266 wave events or rogue waves those in the group whose surface elevation satisfies
 267 $\eta_{\max}(t = 0)/\eta_{\max}(t) \geq 2$. In that way, we can introduce the rogue wave lifetime
 268 which is the duration of the extreme wave event. In figure 9 is shown this duration
 269 as a function of Ω . For positive values of the shear Ω the rogue wave duration is
 270 increased whereas it is the opposite for negative values.

271

272 4 Conclusion

273 The effect of an underlying vortical current on two-dimensional rogue wave prop-
 274 erties has been investigated by using two different approaches in shallow water.
 275 One is based on a new approximate equation, the generalised Whitham equation
 276 with constant vorticity which is fully nonlinear and fully linear dispersive whereas
 277 the other, the BIEM with constant vorticity, is fully nonlinear and fully nonlinear
 278 dispersive. Besides the study on vorticity effect on rogue waves, it is shown that
 279 the results of the generalised Whitham equation with vorticity are in agreement
 280 with those of the BIEM demonstrating that this new single nonlinear equation
 281 is an efficient model for the investigation of nonlinear long waves on vertically
 282 sheared current of constant vorticity.

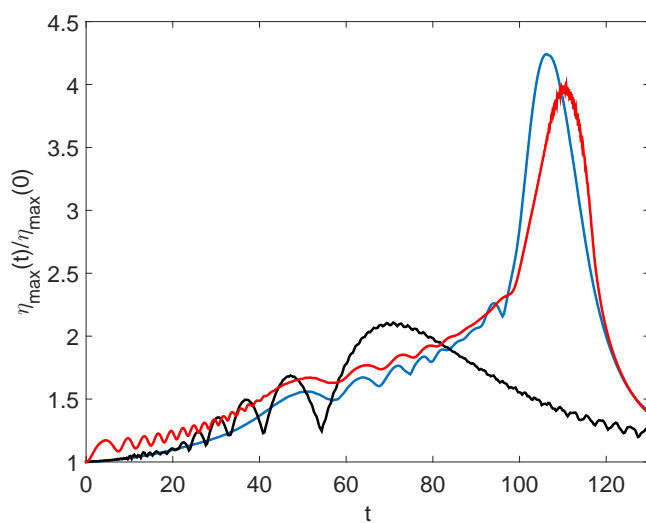


Fig. 4 (color online) Time evolution of the amplification factor with vorticity effect ($\Omega = 0.5$). Generalised Whitam equation (blue solid line), BIEM (red solid line) and KdV equation (black solid line)

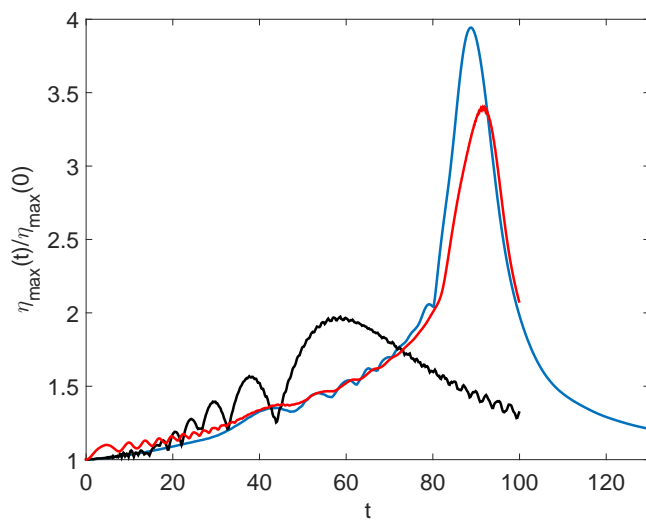


Fig. 5 (color online) Time evolution of the amplification factor with vorticity effect ($\Omega = 0.25$). Generalised Whitam equation (blue solid line), BIEM (red solid line) and KdV equation (black solid line)

283 The numerical simulations carried out with all the approaches have shown that the
 284 presence of vorticity modifies the rogue wave properties significantly. The maxi-
 285 mum of amplification factor of the surface elevation increases as the shear intensity
 286 of the current increases. The lifetime of extreme wave event follows the same ten-
 287 dency.

288 **Appendix**

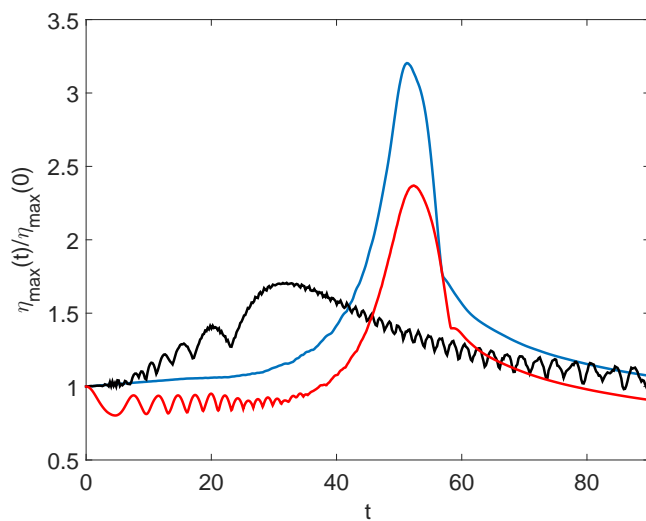


Fig. 6 (color online) Time evolution of the amplification factor with vorticity effect ($\Omega = -0.5$). Generalised Whitham equation (blue solid line), BIEM (red solid line) and KdV equation (black solid line)

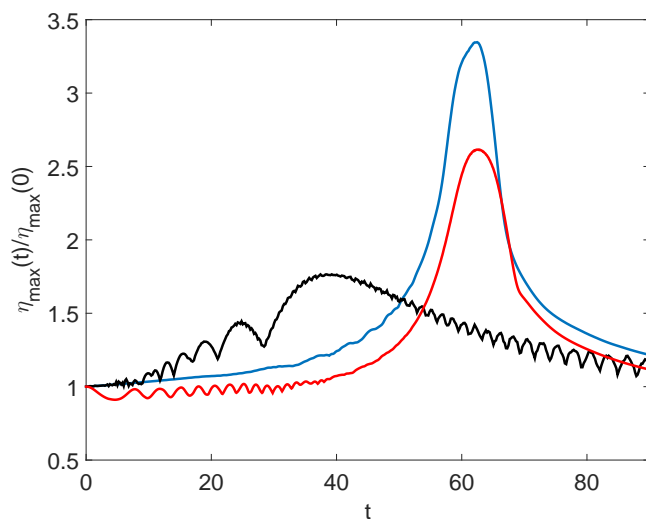


Fig. 7 (color online) Time evolution of the amplification factor with vorticity effect ($\Omega = -0.25$). Generalised Whitham equation (blue solid line), BIEM (red solid line) and KdV equation (black solid line)

289 The pair of equations (3) and (6) admits the following Riemann invariants

$$u + \frac{\Omega H}{2} \pm \left\{ \sqrt{gH + \Omega^2 H^2/4} + \frac{g}{\Omega} \ln \left[1 + \frac{\Omega}{2g} (\Omega H + 2\sqrt{gH + \Omega^2 H^2/4}) \right] \right\} = \text{constant}$$

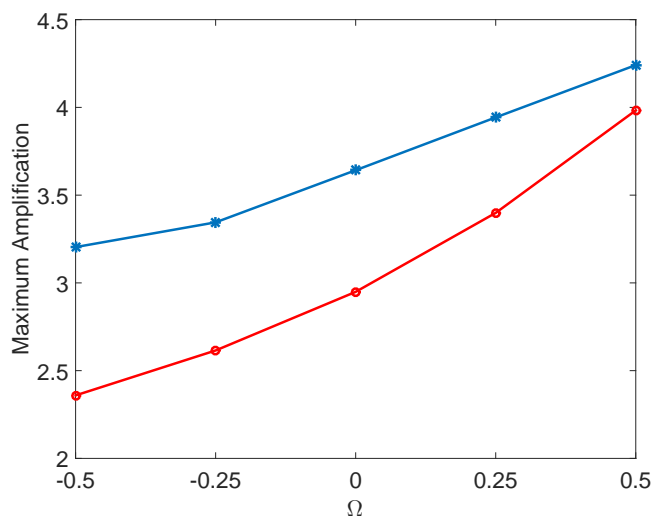


Fig. 8 (color online) Maximum amplification factor at the focusing time as a function of the shear intensity of the current. Generalised Whitam equation (blue solid line), BIEM (red solid line)

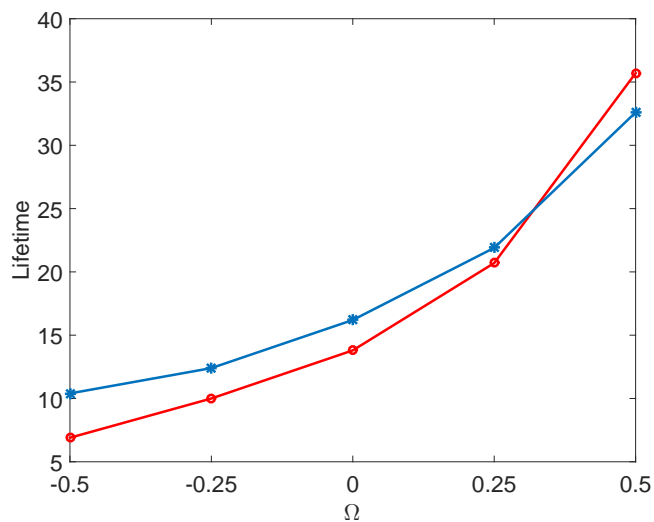


Fig. 9 (color online) Rogue wave duration as a function of the shear intensity of the current. Generalised Whitam equation (blue solid line), BIEM (red solid line)

290 on characteristic lines

$$\frac{dx}{dt} = u + U_0 + \frac{1}{2}\Omega(\eta - h) \pm \sqrt{gH + \frac{\Omega^2 H^2}{4}}$$

291 where $H = \eta + h$.

292 The constant is determined for $u = 0$ and $\eta = 0$ or $H = h$.

293 Finally

$$u + \frac{\Omega\eta}{2} + \sqrt{gH + \Omega^2 H^2/4} - \sqrt{gh + \Omega^2 h^2/4} + \frac{g}{\Omega} \ln \left[\frac{1 + \frac{\Omega}{2g}(\Omega H + 2\sqrt{gH + \Omega^2 H^2/4})}{1 + \frac{\Omega}{2g}(\Omega h + 2\sqrt{gh + \Omega^2 h^2/4})} \right] = 0$$

294

$$u + \frac{\Omega\eta}{2} - \sqrt{gH + \Omega^2 H^2/4} + \sqrt{gh + \Omega^2 h^2/4} - \frac{g}{\Omega} \ln \left[\frac{1 + \frac{\Omega}{2g}(\Omega H + 2\sqrt{gH + \Omega^2 H^2/4})}{1 + \frac{\Omega}{2g}(\Omega h + 2\sqrt{gh + \Omega^2 h^2/4})} \right] = 0$$

295 Let us consider a wave moving rightwards

$$u = -\frac{\Omega\eta}{2} + \sqrt{gH + \Omega^2 H^2/4} - \sqrt{gh + \Omega^2 h^2/4} + \frac{g}{\Omega} \ln \left[\frac{1 + \frac{\Omega}{2g}(\Omega H + 2\sqrt{gH + \Omega^2 H^2/4})}{1 + \frac{\Omega}{2g}(\Omega h + 2\sqrt{gh + \Omega^2 h^2/4})} \right]$$

296 Substituting this expression into equation (3) gives

$$\eta_t + \left\{ U_0 - \frac{\Omega h}{2} + 2\sqrt{g(\eta + h) + \Omega^2(\eta + h)^2/4} - \sqrt{gh + \Omega^2 h^2/4} + \frac{g}{\Omega} \ln \left[1 + \frac{\Omega}{2g} \frac{\Omega\eta + 2(\sqrt{g(\eta + h) + \Omega^2(\eta + h)^2/4} - \sqrt{gh + \Omega^2 h^2/4})}{1 + \frac{\Omega}{g}(\frac{\Omega h}{2} + \sqrt{gh + \Omega^2 h^2/4})} \right] \right\} \eta_x = 0$$

298 This equation is equation (7).

299 **Acknowledgements** The authors would like to thank the French DGA, who supported this
300 work through the ANR grant ANR-13-ASTR-0007.

301 References

- 302 Chambarel J, Kharif C, Kimmoun O (2010) Generation of two-dimensional steep water waves
303 on finite depth with and without wind. *Eur J Mech B/Fluids* 29(2):132–142
304 Choi W (2003) Strongly nonlinear long gravity waves in uniform shear flows. *Phys Rev E*
305 68:026,305
306 Dysthe KI, Krogstad HE, Muller P (2008) Oceanic rogue waves. *Annu Rev Fluid Mech* 40:287–
307 310
308 Freeman N, Johnson R (1970) Shallow water waves on shear flows. *J Fluid Mech* 42 (2):401–409
309 Grimshaw R, Liu Z (2017) Nonlinear periodic and solitary water waves on currents in shallow
310 water. *Studies in Applied Mathematics* pp 1467–9590
311 Hur VM, Johnson MA (2015) Modulational instability in the whitham equation with surface
312 tension and vorticity. *Nonlinear Analysis* 129:104–118
313 Kharif C, Abid M (2017) Whitham approach for the study of nonlinear waves on a vertically
314 sheared current in shallow water. *J Fluid Mech* (in revision)
315 Kharif C, Pelinovsky E (2003) Physical mechanisms of the rogue wave phenomenon. *Eur J*
316 *Mech B/Fluids* 22:603–634
317 Kharif C, Pelinovsky E, Talipova T (2000) Formation de vagues géantes en eau peu profonde.
318 CRAS 328 (Iib):801–807

- 319 Kharif C, Pelinovsky E, Slunyaev A (2009) *Rogue waves in the ocean*. Springer
320 Merkoune D, Touboul J, Abcha N, Mouazé D, Ezersky A (2013) Focusing wave group on a
321 current of finite depth. *Nat Hazards Earth Syst Sci* 13:2941–2949
322 Nwogu OG (2009) Interaction of finite-amplitude waves with vertically sheared current fields.
323 *J Fluid Mech* 627:179–213
324 Onorato M, Residori S, Bertolozzo U, Montina A, Arecchi F (2013) Rogue waves and their
325 generating mechanisms in different physical contexts. *Phys Rep* 528:47–89
326 Pelinovsky E, Sergeeva A (2006) Numerical modeling of kdv random wave field. *Eur J Mech*
327 *B/Fluids* 25:425–434
328 Pelinovsky E, Talipova T, Kharif C (2000) Nonlinear dispersive mechanism of the freak wave
329 formation in shallow water. *Physica D* 147:83–94
330 Peterson P, Soomere T, Engelbrecht J, van Groesen E (2003) Interaction solitons as a possible
331 model for extreme waves in shallow water. *Nonlin Proc Geophys* 10:503–510
332 Simmen JA (1984) Steady deep-water waves on a linear shear current. PhD thesis, California
333 Institute of Technology, Pasadena, Californie
334 Simmen JA, Saffman PG (1985) Steady deep-water waves on a linear shear current. *Stud Appl*
335 *Math* 73:35–57
336 Soomere T, Engelbrecht (2005) Extreme evaluation and slopes of interacting solitons in shallow
337 water. *Wave Motion* 41:179–192
338 Talipova T, Kharif C, Giovanangeli J (2008) Modelling of rogue wave shapes in shallow water.
339 In: *Extreme Ocean Waves*, Springer, Eds. Pelinovsky E. and Kharif C.
340 Toffoli A, Onorato M, Osborne A, Monbaliu J (2006) Non-gaussian properties of surface el-
341 evation in crossing sea states in shallow water. *Proc Int Conf Coast Eng (ICCE06 pp*
342 *782–790*
343 Touboul J, Kharif C (2010) Two-dimensional direct numerical simulations of the dynamics
344 of rogue waves under wind action, *Advances in numerical simulation of nonlinear water*
345 *waves*, vol 11, The world Scientific Publishing Co., London, chap 2
346 Touboul J, Kharif C (2016) Effect of vorticity on the generation of rogue waves due to dispersive
347 focusing. *Natural Hazards* 84(2):585–598
348 Touboul J, Pelinovsky E, Kharif C (2007) Nonlinear focusing wave groups on current. *Journ*
349 *Korean Soc Coast And Ocean Engineers* 19 (3):222–227
350 Whitham G (1974) *Linear and nonlinear waves*. John Wiley & Sons